photonics

MDPI

Article

Three-Dimensional Exploding Light Wave Packets

Marcos G. Barriopedro [1,*], Manuel Holguín [2], Pablo de Lara-Montoya [2], Nilo Mata-Cervera [3] and Miguel A. Porras [1,*]

[1] Complex Systems Group, Escuela Técnica Superior de Minas y Energía (ETSIME), Universidad Politécnica de Madrid, Ríos Rosas 21, 28003 Madrid, Spain
[2] Departamento de Energía y Combustibles, Escuela Técnica Superior de Minas y Energía (ETSIME), Universidad Politécnica de Madrid, Ríos Rosas 21, 28003 Madrid, Spain; manuel.holguin@alumnos.upm.es (M.H.); pablo.delara@alumnos.upm.es (P.d.L.-M.)
[3] Centre for Disruptive Photonic Technologies, School of Physical and Mathematical Sciences & The Photonics Institute, Nanyang Technological University, Singapore 637371, Singapore; nilo001@e.ntu.edu.sg
* Correspondence: m.gbarriopedro@alumnos.upm.es (M.G.B.); miguelangel.porras@upm.es (M.A.P.)

Abstract: We describe a family of paraxial and quasi-monochromatic optical wave packets with finite energy and smoothly shaped amplitude in space and time that develops a singularity in the intensity when spatio-temporally focused by imparting a converging spherical wavefront and a negative temporal chirp. This singular behavior upon ideal focusing is manifested in actual focusing with finite apertures and in media with high-order dispersion with "exploding" behavior featuring an indefinitely increasing concentration of the energy when opening the aperture radius, thus exercising continuous control on the focal intensity and spatial and temporal resolution. These wave packets offer a new way of focusing that outperforms what can be achieved with standard Gaussian wave packets in terms of focal intensity and resolution, providing new possibilities in applications where energy concentration and its control are crucial.

Keywords: structured light; beam shaping; pulse shaping; ultrafast optics

Citation: Barriopedro, M.G.; Holguín, M.; de Lara-Montoya, P.; Mata-Cervera, N.; Porras, M.A. Three-Dimensional Exploding Light Wave Packets. *Photonics* **2024**, *11*, 652. https://doi.org/10.3390/photonics11070652

Received: 22 May 2024
Revised: 1 July 2024
Accepted: 8 July 2024
Published: 11 July 2024

1. Introduction

Structured light has gained attraction in recent years, and is now one of the central research directions in photonics. The ultimate goal is to explore all degrees of freedom of light to tailor arbitrary optical fields. In the basic scenario of monochromatic fields, complex amplitude and polarization manipulation are the domain of modern photonic technologies such as spatial light modulators [1], digital micromirror devices [2], metamaterials [3], etc. At its simplest, shaping amplitude and phase in a certain polarization state is essential to realize arbitrary scalar beams, where the vectorial feature of light plays no role. This is the case with well-known free-space eigenmodes such as Laguerre–Gaussian (LG) and Hermite–Gaussian beams [4], Airy beams [5], Ince–Gaussian beams [6] etc. By further combining orthogonal polarization states, complex vector beams with inhomogeneous polarisation textures are obtained, such as radial/azimuthal cylindrical vector beams [7], full Poincaré beams [8], optical skyrmions [9], etc.

The present work concerns broader context of spatio-temporal light shaping, which involves sculpturing the properties of light fields simultaneously in the spatial and temporal (spectral) domains. Compared to monochromatic fields, or space–time separable fields, non-separable spatio-temporal light fields feature radically different behaviors [10], which have been studied in various contexts such as toroidal electrodynamics and anapole radiation [11,12], spatio-temporal vortices [13,14], scalar hopfions [15], etc.

A recent trend in structured light is singular beams, initially monochromatic beam solutions of the Schrödinger equation for paraxial propagation in non-dispersive media that yield singular (infinite) focal intensity under ideal focusing conditions, mimicking

focusing of a plane wave but with finite power. In this context, one-dimensional "concentrating" beams were first described in [16] and later observed in experiments in [17]. This was followed by two-dimensional exploding beams and vortex beams with cylindrical symmetry [18] and their recent experimental realization using metasurfaces [19]. Although singularity only appears under ideal conditions, in real settings, singular beams provide much larger peak intensities and finer spatial resolutions than other standard beams with the same power, which is of great interest in areas such as atom trapping [20], microscopy [21], material processing [22], etc. Indeed, concentrating electromagnetic energy in minimal spots has been investigated since the invention of lasers and the development of beam shaping techniques [23], from binary optics [24] all the way to the present day with approaches such as superoscillatory fields [25]. Along with revolutionary pulse amplification techniques [26,27] with which modern pulsed laser systems have achieved powers up to 10^{15} W and peak intensities of 10^{23} W/cm^2 [28], shaping the beam and pulse degrees of freedom is crucial to reach even higher levels.

In the present work, we continue previous research on singular fields and extend the concept to the three-dimensional, spatio-temporal domain, describing what we call exploding wave packets (EWPs) with non-separable, spatio-temporal spherical symmetry. These EWPs are finite-energy analytical solutions to the paraxial diffraction integral or the linear Schrödinger equation in second-order dispersive media that develop a singular (infinite) intensity when they are ideally spatio-temporally focused, i.e., focused spatially and compressed temporally. As for its predecessors, the ideal singularity disappears under real focusing conditions with finite apertures and in media with high-order dispersion. Nevertheless, the existence of ideal singularity has physical manifestations such as a continuous increase in the focal intensity and a continuous diminution in the transversal spot size with increasing aperture radius that makes them arbitrarily improve the focusing capabilities of standard Gaussian wave packets under similar conditions of peak intensity and energy. High-order dispersion sets a limit to the minimum duration; nevertheless, this duration is substantially smaller than that achievable with Gaussian pulses.

Note that, as with preceding singular beams [16–19], we do not resort here to strong, non-paraxial focusing with large numerical apertures but, instead, we focus on paraxial focusing to emphasize the focusing properties of the spatio-temporally shaped exploding profile itself through its analytical properties. In fact, all our examples are fully paraxial. As pointed out in [19], non-paraxial focusing of exploding beams yields an even stronger concentration of energy.

2. Methods

2.1. Propagation of Spatio-temporal Symmetric Wave Packets in Dispersive Media

We consider a quasi-monochromatic pulsed beam $E = \psi e^{-i\omega_0 t + ik_0 z}$ of carrier frequency ω_0 and propagating along the z direction, whose complex envelope ψ is governed by the Schrödinger equation.

$$\frac{\partial \psi}{\partial z} = \frac{i}{2k_0}\Delta_\perp \psi - \frac{ik_0''}{2}\frac{\partial^2 \psi}{\partial t'^2}, \tag{1}$$

where $\Delta_\perp = \partial^2/\partial x^2 + \partial^2/\partial y^2$, k_0 is the propagation constant at the carrier frequency, k_0'' is the GVD, t' is the local time $t' = t - k_0' z$, and $1/k_0'$ is the group velocity. Assuming anomalous dispersion ($k_0'' < 0$), we introduce the time $\tau = t'/\sqrt{k_0|k_0''|}$ with units of length, and Equation (1) becomes the following:

$$\frac{\partial \psi}{\partial z} = \frac{i}{2k_0}\left(\frac{\partial^2 \psi}{\partial x^2} + \frac{\partial^2 \psi}{\partial y^2} + \frac{\partial^2 \psi}{\partial \tau^2}\right). \tag{2}$$

The propagator of Equation (2) that yields the propagated envelope of an arbitrary illumination $\psi(x', y', \tau', 0)$ has a well-known analogous in the quantum mechanics of a free particle, and reads here as a Fresnel diffraction integral generalized to three dimensions:

$$\begin{aligned}\psi(x,y,\tau,z) &= \left(\frac{k_0}{2\pi i z}\right)^{3/2} \int_{\mathbb{R}^3} \psi(x',y',\tau',0) e^{\frac{ik_0}{2z}\left[(x-x')^2+(y-y')^2+(\tau-\tau')^2\right]} dx'dy'd\tau' \\ &= \left(\frac{k_0}{2\pi i z}\right)^{3/2} e^{\frac{ik_0}{2z}(x^2+y^2+\tau^2)} \\ &\times \int_{\mathbb{R}^3} \psi(x',y',\tau',0) e^{-\frac{ik_0}{z}(xx'+yy'+\tau\tau')} e^{\frac{ik_0}{2z}(x'^2+y'^2+\tau'^2)} dx'dy'd\tau'. \end{aligned} \tag{3}$$

We consider wave packets whose complex envelope only depend on $r = (x^2 + y^2 + \tau^2)^{1/2}$, which we will call a spatio-temporal spherically symmetric wave packet. For these wave packets, the Schrödinger Equation (2) can be written as follows:

$$\frac{\partial \psi}{\partial z} = \frac{i}{2k_0} \frac{1}{r^2} \frac{\partial}{\partial r}\left(r^2 \frac{\partial \psi}{\partial r}\right), \tag{4}$$

which implies that symmetry is preserved on propagation. The propagator in Equation (3) can be simplified accordingly. We introduce spatio-temporal spherical coordinates $x = r\sin\phi\cos\theta$, $y = r\sin\phi\sin\theta$, and $\tau = r\cos\phi$, (similar for x', y', and τ') to rewrite Equation (3) as follows:

$$\begin{aligned}\psi(r,z) &= \left(\frac{k_0}{2\pi i z}\right)^{3/2} e^{\frac{ik_0}{2z}r^2} \int_0^\infty \psi(r',0) e^{\frac{ik_0}{2z}r'^2} r'^2 dr' \int_0^\pi e^{-\frac{ik_0}{z}rr'\cos\phi\cos\phi'} \sin\phi' d\phi' \\ &\times \int_0^{2\pi} e^{-\frac{ik_0}{z}rr'\sin\phi\sin\phi'\cos(\theta-\theta')} d\theta'. \end{aligned} \tag{5}$$

The integral in θ' is $2\pi J_0(k_0 rr'\sin\phi\sin\phi'/z)$, where $J_0(\cdot)$ is the Bessel function of the first kind and order zero, which introduced in Equation (5) provides the following:

$$\begin{aligned}\psi(r,z) &= 2\pi\left(\frac{k_0}{2\pi i z}\right)^{3/2} e^{\frac{ik_0}{2z}r^2} \int_0^\infty \psi(r',0) e^{\frac{ik_0}{2z}r'^2} r'^2 dr' \\ &\times \int_0^\pi e^{-\frac{ik_0}{z}rr'\cos\phi\cos\phi'} J_0\left(\frac{k_0 rr'}{z}\sin\phi\sin\phi'\right)\sin\phi' d\phi'. \end{aligned} \tag{6}$$

In the last integral, only the cosine of the exponential contributes. Since the spatio-temporal symmetry is preserved, the integral in ϕ' must be independent of ϕ, and it can conveniently be evaluated with $\phi = 0$, i.e.,

$$\int_0^\pi \cos\left(\frac{k_0}{z}rr'\cos\phi'\right)\sin\phi' d\phi' = \frac{2z}{k_0 rr'}\sin\left(\frac{k_0 rr'}{z}\right). \tag{7}$$

Introducing Equation (7) into Equation (6) we obtain the following:

$$\psi(r,z) = 4\pi\left(\frac{k_0}{2\pi i z}\right)^{\frac{3}{2}} e^{i\frac{k_0 r^2}{2z}} \int_0^\infty \psi(r',0) e^{\frac{ik_0}{2z}r'^2} \operatorname{sinc}\left(\frac{k_0 rr'}{z}\right) r'^2 dr', \tag{8}$$

where $\operatorname{sinc}\alpha \equiv \sin\alpha/\alpha$ and provides the simplified form of the propagator for spatio-temporal spherically symmetric wave packets in the dispersive medium.

Let us choose $\psi(r,0) = \psi(r)e^{-ik_0 r^2/2f}$, where $\psi(r)$ is real. Displaying the exponential $e^{-ik_0 r^2/2f}$ as $e^{-ik_0 r^2/2f} = e^{-ik_0(x^2+y^2)/2f} e^{-it'^2/2f|k_0''|}$, it is evident that $\psi(r)e^{-ik_0 r^2/2f}$ represents focusing on the illumination $\psi(r)$ with focal length $f > 0$ and a negative chirp

$-1/2f|k_0''|$ spatio-temporally in such a way that the spatio-temporal spherical symmetry is preserved. Equation (8) then becomes

$$\psi(r,z) = 4\pi\left(\frac{k_0}{2\pi i z}\right)^{\frac{3}{2}} e^{i\frac{k_0 r^2}{2z}} \int_0^\infty \psi(r') e^{\frac{ik_0}{2}r'^2\left(\frac{1}{z}-\frac{1}{f}\right)} \mathrm{sinc}\left(\frac{k_0 r r'}{z}\right) r'^2 dr', \tag{9}$$

and at the focal plane $z = f$,

$$\psi(r,f) = 4\pi\left(\frac{k_0}{2\pi i f}\right)^{\frac{3}{2}} e^{i\frac{k_0 r^2}{2f}} \int_0^\infty \psi(r') \mathrm{sinc}\left(\frac{k_0 r r'}{f}\right) r'^2 dr', \tag{10}$$

which provides the spatio-temporally focused field.

2.2. Ideal Exploding Wave Packets

Let the illuminating wave packet be

$$\psi(r) = \sqrt{\frac{E}{C}}\left[\frac{1}{1+r^2/\beta^2}\right]^{\mu+1/2} = \sqrt{\frac{E}{C}}\left[\frac{1}{1+(x^2+y^2)/\beta^2 + t'^2/(k_0|k_0''|\beta^2)}\right]^{\mu+1/2}, \tag{11}$$

where β determines the spatial size and temporal duration $\Delta t = \sqrt{k_0|k_0''|}\beta$. If $\mu > 1/4$, then the energy of this wave packet is finite; therefore, the wave packet is physically realizable. If we choose $C = \sqrt{k_0|k_0''|}\pi^{3/2}\beta^3\Gamma(2\mu-1/2)/\Gamma(2\mu+1)$ in Equation (11), where $\Gamma(\cdot)$ is the gamma function, it can be readily seen that E in Equation (11) coincides with the finite energy carried by the wave packet, i.e., $E = \int dxdydt'|\psi|^2 = 4\pi\sqrt{k_0 k_0''}\int_0^\infty drr^2|\psi(r)|^2$. Fitting Equation (11) into Equation (10) yields optical disturbance at the focal plane. The resulting integral can be performed analytically using integral 3.251.2 in Ref. [29], obtaining, after some algebra,

$$\psi(r,f) = \sqrt{\frac{E}{C}}\beta^{\mu+2}\frac{2}{\pi}\left(\frac{1}{ir}\right)^{\frac{3}{2}} e^{i\frac{k_0 r^2}{2f}} \left(\frac{k_0 r}{2f}\right)^{\mu+\frac{1}{2}} \cos(\pi\mu)\Gamma\left(\frac{1}{2}-\mu\right) K_{1-\mu}\left(\frac{k_0\beta r}{f}\right), \tag{12}$$

where $K_\nu(\cdot)$ is the modified Bessel function of the second kind and order ν. Considering the asymptotic behavior of $K_\nu(\alpha) \simeq (1/2)\Gamma(\nu)(\alpha/2)^{-\nu}$ for small values of α, the field at the focus $r = 0$ is seen to present a singularity, $\psi \to \infty$, when $r \to 0$, if $\mu < 1$. In short, if we take the parameter μ, or the decay parameter, in the range

$$1/4 < \mu < 1, \tag{13}$$

the input illumination in Equation (11) carries finite energy and produces a focused field with infinite intensity at the focus. Note that, for $\mu = 1/2$, the singularity of the gamma function is removed by the zero of the cosine; indeed, $\cos(\pi\mu)\Gamma(1/2-\mu) = \pi$ for $\mu = 1/2$. In addition, the use of $K_{1/2}(\alpha) = \sqrt{\pi/(2\alpha)}e^{-\alpha}$ leads to a simpler expression:

$$\psi(r,f) = \sqrt{\frac{E}{C}}\beta^2(-i)^{3/2}\sqrt{\frac{\pi k_0}{2f}} e^{i\frac{k_0 r^2}{2f}} \frac{1}{r} e^{-\frac{k_0\beta r}{f}}, \tag{14}$$

for $\mu = 1/2$. Figure 1a,b shows an example of the EWP spatio-temporal radial profile in Equation (11) at $z = 0$ and the focal plane in Equation (14), respectively, in fused silica at a wavelength with second-order anomalous dispersion. How it looks in real space–time is shown in Figure 1c,d. They are compared with spatio-temporal spherically symmetric Gaussian wave packets of the same peak intensity and energy, $\psi = \sqrt{E/C}e^{-r^2/w^2}e^{-ik_0 r^2/2f}$, that are spatio-temporally focused in the same way, where the choice $w^3 = 4C/\sqrt{k_0|k_0''|2\pi^3}$ equates to the energies.

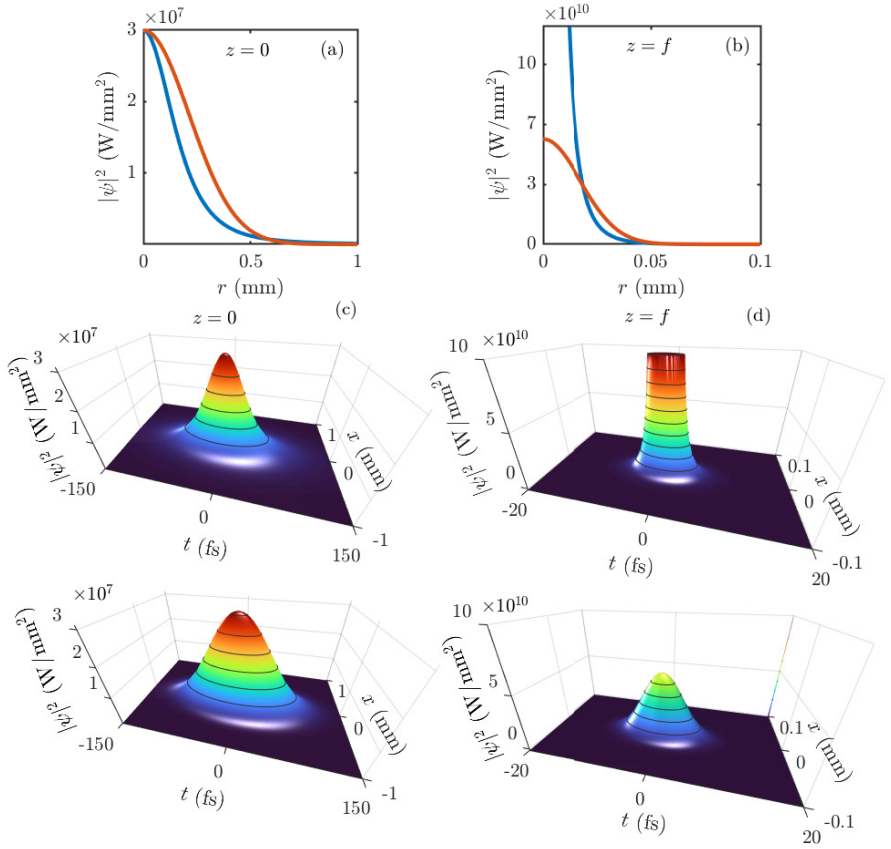

Figure 1. EWP at $\omega_0 = 1.4$ rad/fs ($\lambda_0 = 1.346$ μm) ideally focused in fused silica ($k_0 = 6754$ mm^{-1}, $k_0' = 4876$ fs mm^{-1}, $k_0'' = -6.508$ fs^2 mm^{-1}). (**a**) Spatio-temporal radial intensity profile of the EWP (blue) with $\beta = 0.25$ mm and $\mu = 1/2$, and of the Gaussian wave packet (orange) with $w = 0.428$ mm of the same peak intensity and energy $E = 1$ μJ. (**b**) Their focused intensity profiles with f = 50 mm. (**c**) The same EWP (top) and Gaussian wave packet (bottom) in space and real-time with a width of duration $\Delta t = \sqrt{k_0|k_0''|\beta} = 104.8$ fs. (**d**) Their focused intensity profiles. The different colors represent the different values of the intensity specified in the vertical axes in (**c**,**d**).

Figure 2 shows the on-axis intensity as it grows up to infinity to verify that the singularity is only formed at the focal plane and to compare it with the on-axis intensity of the Gaussian wave packet of the same intensity and energy. We note that, for the chosen parameters, there is a small focal shift for the Gaussian wave packet. The on-axis intensity of the EWP is also slightly asymmetric, but the singularity is only formed at the focal plane $z = f$.

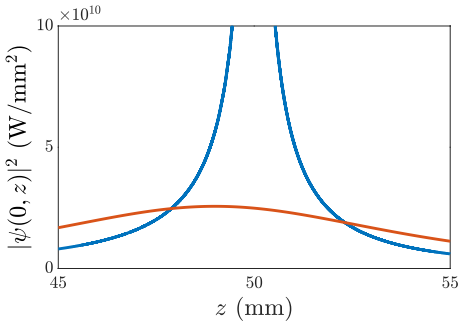

Figure 2. On-axis intensity of the same EWP (blue) and Gaussian wave packet (orange) as in Figure 1 as functions of propagation distance z.

2.3. Real Exploding Wave Packets

The above is, of course, a description of an ideal situation where aperture and high-order dispersion effects are ignored. However, as described in the Results and Discussion Sections, the ideal singularity has real manifestations in actual spatio-temporal focusing, manifestations that we have called exploding behavior [18].

Our results for apertured systems in real media will be obtained from a realistic model of pulsed beam propagation. First, the circular aperture breaks the spatio-temporal spherical symmetry of the exploding illumination, and only cylindrical symmetry in space remains. Second, in order to take into account the effects of high-order dispersion effects properly, we consider the temporal frequency spectrum $\hat{E}(\rho,\omega,0) = (1/2\pi)\int_{-\infty}^{\infty} E(\rho,t,0)e^{i\omega t}dt$ of the exploding illumination $E(\rho,t,0) = \psi(\rho,t,0)e^{-i\omega_0 t}$:

$$\psi(\rho,t,0) = \sqrt{\frac{E}{C}}\left[\frac{1}{1+\rho^2/\beta^2+t^2/(k_0|k_0''|\beta^2)}\right]^{\mu+1/2} e^{-it^2/2f|k_0''|}, \tag{15}$$

where $\rho = \sqrt{x^2+y^2}$, including the temporal chirp in the last factor. Then, we propagate each frequency from the focusing lens of finite radius R towards the focus, as described by the Fresnel diffraction integral for cylindrically symmetric beams [18] with the exact propagation constant $k(\omega) = n(\omega)(\omega/c)$, where $n(\omega)$ is the refractive index of the medium, namely,

$$\hat{E}(\rho,\omega,z) = e^{ik(\omega)z}\frac{k(\omega)}{iz}e^{\frac{ik(\omega)\rho^2}{2z}}\int_0^R d\rho'\rho'\hat{E}(\rho',\omega,0)e^{\frac{ik(\omega)\rho'^2}{2}\left(\frac{1}{z}-\frac{1}{f}\right)}J_0\left[\frac{k(\omega)\rho\rho'}{z}\right], \tag{16}$$

where the focusing of each monochromatic component is accounted for by factor $e^{\frac{-ik(\omega)\rho'^2}{2f}}$, and then, returns to the time domain $E(\rho,t,z) = \int_{-\infty}^{\infty}\hat{E}(\rho,\omega,z)e^{-i\omega t}d\omega$.

For numerical computation, it is convenient to evaluate the envelope $\psi(\rho,t',z)$ of $E(\rho,t,z) = \psi(\rho,t',z)e^{-i\omega_0 t+ik_0 z}$ in the local time, given by $\psi(\rho,t',z) = \int_{-\infty}^{\infty} d\Omega\hat{\psi}(\rho,\Omega,z)e^{-i\Omega t'}$, where $\Omega = \omega-\omega_0$:

$$\begin{aligned}\hat{\psi}(\rho,\Omega,z) &= e^{i[k(\omega_0+\Omega)-k_0-k_0'\Omega]z}\frac{k(\omega_0+\Omega)}{iz}e^{\frac{ik(\omega_0+\Omega)\rho^2}{2z}}\\ &\times \int_0^R d\rho'\rho'\hat{\psi}(\rho',\Omega,0)e^{\frac{ik(\omega_0+\Omega)\rho'^2}{2}\left(\frac{1}{z}-\frac{1}{f}\right)}J_0\left[\frac{k(\omega_0+\Omega)\rho\rho'}{z}\right],\end{aligned} \tag{17}$$

and $\hat{\psi}(\rho,\Omega,0) = (1/2\pi)\int_{-\infty}^{\infty} dt\psi(\rho,t,0)e^{i\Omega t}$ is the Fourier transform of the input envelope.

3. Results

As announced, the singularity of ideal EWPs is not observed with real EWPs delivered by focusing systems with finite aperture in materials with high-order dispersion. However, it turns out that the theoretical existence of the ideal singularity has physical, observable consequences that make EWPs feature unconventional focusing properties compared to standard wave packets, such as a Gaussian wave packet in space and time. In the following, we always compare the focusing performance of real EWPs with that of a spatio-temporal symmetric Gaussian wave packet with the same peak intensity on the input plane of the focusing system and equal energy. This is the fairest comparison when evaluating the focusing capabilities of two wave packets with different spatio-temporal profiles. Our results clearly demonstrate that, with sufficiently large aperture, EWPs always outperform the capability of Gaussian wave packets to concentrate the energy in space and time, i.e., produce higher peak intensity in smaller focal spots and shorter pulses.

For a realistic set of parameters of an EWP in the infrared spectrum and in fused silica, Figure 3a–c shows that the peak intensity at the focus $[(\rho,z) = (0,f)]$ grows without bound towards the ideal singularity with increasing aperture, while the peak intensity of the Gaussian wave packet does not experience any change once the aperture is larger than

approximately twice its spot size w. In Figure 4a–c, the double vertical scale for the EWP and the Gaussian wave packet helps to evidence that the EWP shrinks transversally without bound at the focal plane (ρ, f) as the aperture is opened, outperforming the Gaussian wave packet in transversal resolution, which does not experience any change once the aperture is sufficiently opened. The behavior of the peak intensity and of the transversal spot size is summarized in Figure 5a,b, where they are plotted for EWPs of different decay parameters μ as functions of the aperture radius and compared to the same properties for Gaussian wave packets.

H

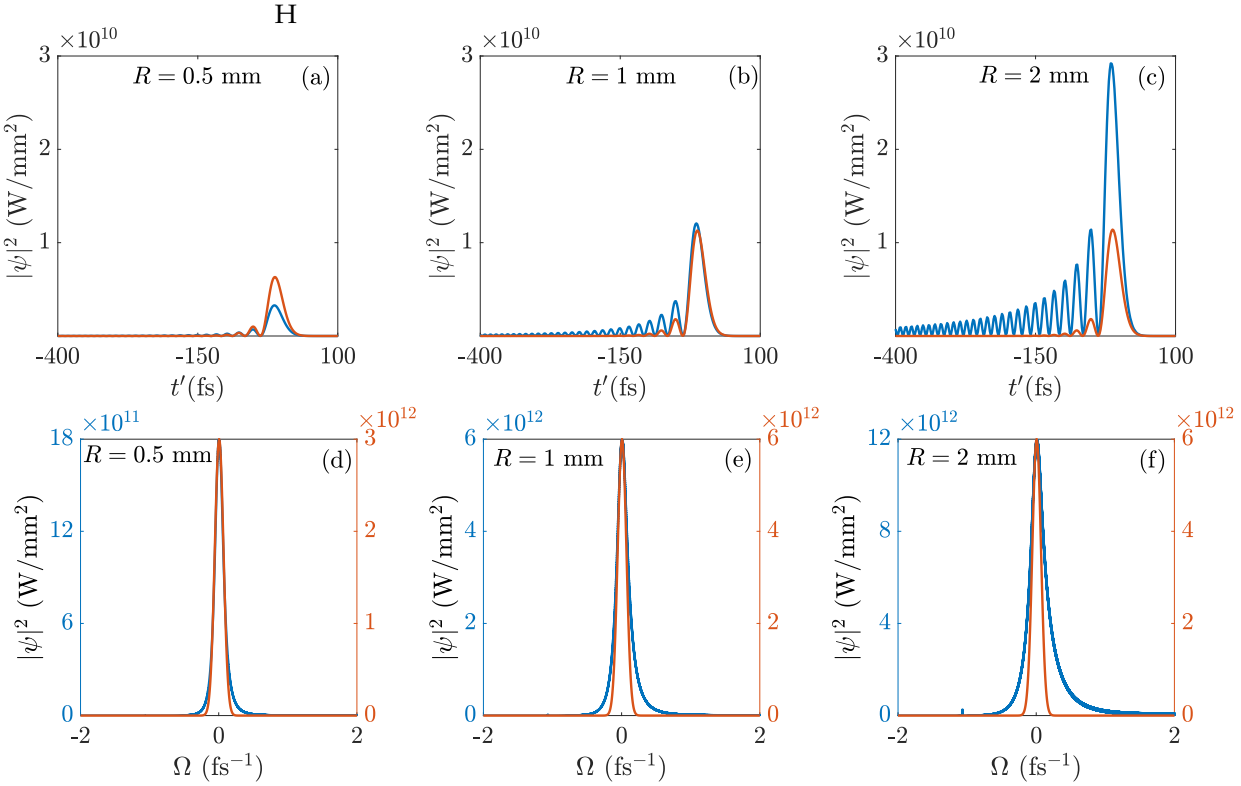

Figure 3. EWP at $\omega_0 = 1.2$ rad/fs ($\lambda_0 = 1.57$ μm) focused in fused silica modeled by a Sellmeier relation with three resonances. Comparison between the temporal shape at the focus of the EWP with $\mu = 1/2$ and $\beta = 0.25$ (blue) and a Gaussian wave packet (orange) of the same initial peak intensity and the same energy with ($w = 0.428$ mm) when the raddi of the aperture are $R = 0.5$ mm (**a**), $R = 1$ mm (**b**), and $R = 2$ mm (**c**). Comparison between the respective temporal frequency spectral densities is shown in (**d**–**f**). The double vertical scales help to compare the spectral widths.

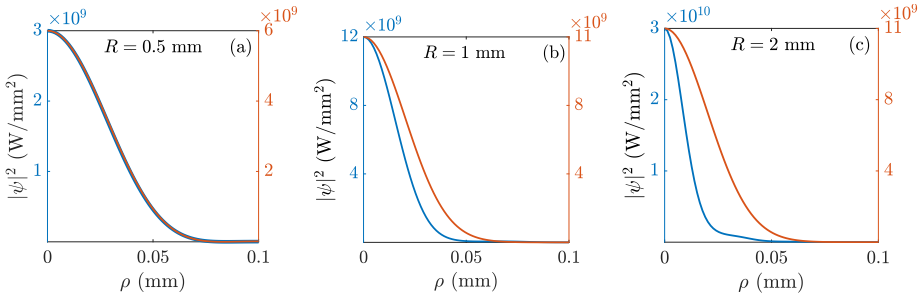

Figure 4. EWPs at $\omega_0 = 1.2$ rad/fs ($\lambda = 1.57$ μm) focused in fused silica modeled by a Sellmeier relation with three resonances. Comparison between the radial profiles at the focal plane at instant of time of maximum intensity of the EWP with $\mu = 0.5$ and $\beta = 0.25$ (blue) and of the Gaussian wave packet (orange) of the same initial peak intensity and energy when the aperture radii are $R = 0.5$ mm (**a**), $R = 1$ mm (**b**), and $R = 2$ mm (**c**).

As for the temporal duration at the focus $[(\rho, z) = (0, f)]$, third and high-order dispersion set a limit to the minimum achievable duration for both the EWP and the Gaussian wave packet, but still, the EWP reached a significantly shorter duration. Here, it is important to note the peculiarity that the spatio-temporal spherical Gaussian wave packet is at the same time separable in space and time, where focus and dispersion can be described from two separate Schrödinger Equations (1) with only the diffraction and dispersion terms. This is why opening the aperture has no effect on the temporal-frequency spectrum at the focus, as seen in Figure 3d–f. In contrast, the spherical symmetric EWP is not separable in space and time. The wider and broadening spectra observed in Figure 3d–f can only be attributed to its non-separability. In the time domain, this fact leads to a minimum achievable duration smaller than the minimum achievable duration of the Gaussian wave packet. This unique property is illustrated in Figure 5c, where the duration at the focus of EWPs with different decay parameters μ is seen to approach minimum values smaller than the constant values of the respective Gaussian wave packets of the same peak intensity and energy.

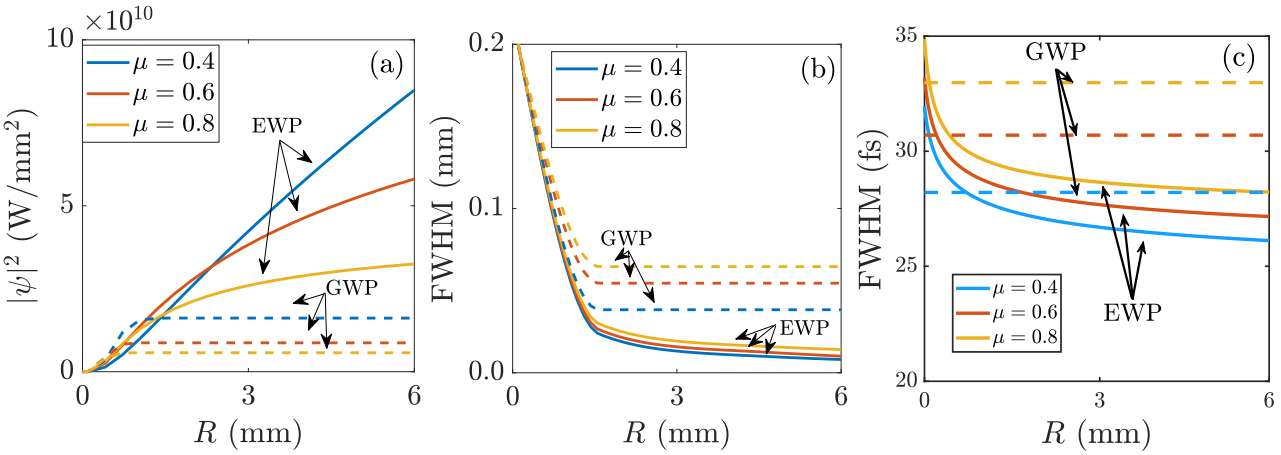

Figure 5. Properties of EWPs at $\omega_0 = 1.2$ rad/fs ($\lambda = 1.57$ μm) and $\beta = 0.25$ mm focused in fused silica modeled by a Sellmeier relation with three resonances. (**a**) Peak intensity for the indicated values of the decay parameter μ as a function of the radius of the aperture R, compared to the same property for Gaussian wave packets of the same peak intensity and energy. (**b**) Radial FWHM of the same EWPs and Gaussian wave packets as functions of R. (**c**) Temporal FWHM of the EWPs and Gaussian wave packets as functions of R.

4. Discussion

Here, we present a comparison with similar work. As stated in the Introduction, our results extend the exploding behavior of the 2D exploding monochromatic beam [18,19] to 3D. Similar exploding behavior would also be present in a pulsed, instead of the monochromatic, 2D exploding beam by multiplying the monochromatic one by a temporal envelope such as a Gaussian envelope. In that case, the minimum achievable duration would be that of the horizontal dashed lines in Figure 5c. Instead, the non-separable profile of the EWP sets a lower minimum duration, represented by the solid curves in Figure 5c.

Of course, the EWP does not produce the highest concentration of energy in an absolute sense. The same peak intensity on the focusing system and the same energy are crucial for a fair comparison with the Gaussian wave packet. For example, maintaining the peak intensity and increasing the Gaussian width tend to fill the aperture, so approaching the diffraction limit will produce a tighter and more intense focus, but this procedure increases the energy of the Gaussian wave packet. To be fair, we should also increase the EWP parameter β to equate the energies and, again, with further increase in the aperture, the EWP will outperform the wider Gaussian wave packet, which, in turn, may once again be enlarged to fill the new aperture, and so on.

However, this "reshaping" procedure is costly experimentally and, more importantly, is alien to the idea of explosive behavior, whose main features are as follows: (a) the EWP mimics, with *finite energy* , focusing of an ideal, unfeasible plane wave *with infinite energy* . In both cases, the focal spot is narrower and more intense when the aperture is opened. (b) We chose the same peak intensity and energy to fix a set of parameters for a reasonably fair comparison. Actually, *without resorting to any reshaping procedure,* the focusing capability of EWPs always outperforms that of any standard Gaussian-like wave packet for sufficiently large aperture since the EWP approaches, without bound, the ideal singularity, while the exponentially decaying tails of a Gaussian wave packet quickly stop contributing to shaping the focused wave packet. This property entails a continuous control of the focal properties using a unique illuminating field.

It is important to notice that the finiteness of the energy, or mathematically, the convergence of the integral $E = \int dxdydt'|\psi|^2$ for the EWP, implies that the encircled energy does not significantly change when opening the aperture several times β. The increase in the peak intensity originates instead from the constructive interference effect of the enlarging encircled EWP periphery carrying increasingly negligible energy.

5. Conclusions

In conclusion, we have described a spatio-temporal light wave packet carrying finite energy and a physically realizable wave packet that ideally develops a singularity in its intensity when focused in space and time in a medium with anomalous group velocity dispersion, and have studied the real-world manifestations of such a singular behavior. The concentration of the focused energy can be increased as desired with the same illuminating wave packet just by increasing the aperture radius of the focusing system. In contrast to previous works, the concentration of the energy takes place in all dimensions, i.e., (x, y, t'), or equivalently, (x, y, z).

The spontaneous development of singularity resembles the phenomenon of collapse in nonlinear Kerr-type media. However, this phenomenon occurs here in a linear medium and, therefore, occurs independently of the energy of the wave packet. In fact, the exploding wave packet is a solution of the linear Schrödinger equation in the third dimension, and as such, the same wave packet is of interest not only in optics but in other fields of physics such as quantum mechanics or acoustics.

In reference to the experimental aspects of optics, developing a spatio-temporally symmetric wave packet in the laboratory presents some difficulty. These include precise pulse shaping and control over temporal dispersion. Recent progress in metamaterial design [12] provides a powerful tool to manipulate space–time-coupled ultrashort pulses, which could be of great interest for the experimental realization of EWPs. Maintaining phase coherence and intensity modulation is crucial, as interactions with the propagation medium, such as noise or non-linear effects, can induce alterations to the properties of these wave packets. Nevertheless, the novel capability properties of EWP in three dimensions would find application in linear or nonlinear optics experiments where exercising precise and continuous control of the focal spot and its intensity of the three-dimensional focal spot field are crucial, particularly in laser surgery, particle trapping, and material processing.

Author Contributions: M.A.P. conceived the idea and supervised the work. M.G.B., M.H., P.d.L.-M., N.M.-C. and M.A.P. have contributed equally in methodology, software, validation, formal analysis, writing and visualization. All authors have read and agreed to the published version of the manuscript.

Funding: Funding was received from the Spanish Ministry of Science and Innovation, Gobierno de España, Contract No. PID2021-122711NB-C21.

Data Availability Statement: Data underlying the results presented in this paper are not publicly available at this time but may be obtained from the authors upon reasonable request.

Acknowledgments: This work was partially supported by the Spanish Ministry of Science and Innovation, Gobierno de España, under Contract No. PID2021-122711NB-C21. P.d.L.-M. and M.H.

acknowledge support from Grant No. D480 (Beca de colaboración de formación) of the Universidad Politécnica de Madrid.

Conflicts of Interest: The authors declare no conflicts of interest.

References

1. Efron, U. *Spatial Light Modulator Technology: Materials, Devices, and Applications*; CRC Press: Boca Raton, FL, USA, 1994; Volume 47.
2. Hu, X.B.; Rosales-Guzmán, C. Generation and characterization of complex vector modes with digital micromirror devices: A tutorial. *J. Opt.* **2022**, *24*, 034001. [CrossRef]
3. Brener, I.; Liu, S.; Staude, I.; Valentine, J.; Holloway, C. *Dielectric Metamaterials: Fundamentals, Designs and Applications*; Woodhead Publishing: Sawston, UK, 2019.
4. Saleh, B.E.; Teich, M.C. *Fundamentals of Photonics*; John Wiley & Sons: Hoboken, NJ, USA, 2019.
5. Siviloglou, G.; Broky, J.; Dogariu, A.; Christodoulides, D. Observation of accelerating airy beams. *Phys. Rev. Lett.* **2007**, *99*, 213901. [CrossRef]
6. Bandres, M.A.; Gutiérrez-Vega, J.C. Ince–gaussian beams. *Opt. Lett.* **2004**, *29*, 144–146. [CrossRef]
7. Zhan, Q. Cylindrical vector beams: From mathematical concepts to applications. *Adv. Opt. Photonics* **2009**, *1*, 1–57. [CrossRef]
8. Beckley, A.M.; Brown, T.G.; Alonso, M.A. Full poincaré beams. *Opt. Express* **2010**, *18*, 10777–10785. [CrossRef] [PubMed]
9. Shen, Y.; Zhang, Q.; Shi, P.; Du, L.; Yuan, X.; Zayats, A.V. Optical skyrmions and other topological quasiparticles of light. *Nat. Photonics* **2024**, *18*, 15–25. [CrossRef]
10. Shen, Y.; Zhan, Q.; Wright, L.G.; Christodoulides, D.N.; Wise, F.W.; Willner, A.E.; Zou, K.h.; Zhao, Z.; Porras, M.A.; Chong, A.; et al. Roadmap on spatiotemporal light fields. *J. Opt.* **2023**, *25*, 093001. [CrossRef]
11. Papasimakis, N.; Fedotov, V.; Savinov, V.; Raybould, T.; Zheludev, N. Electromagnetic toroidal excitations in matter and free space. *Nat. Mater.* **2016**, *15*, 263–271. [CrossRef] [PubMed]
12. Zdagkas, A.; McDonnell, C.; Deng, J.; Shen, Y.; Li, G.; Ellenbogen, T.; Papasimakis, N.; Zheludev, N.I. Observation of toroidal pulses of light. *Nat. Photonics* **2022**, *16*, 523–528. [CrossRef]
13. Wan, C.; Chong, A.; Zhan, Q. Optical spatiotemporal vortices. *eLight* **2023**, *3*, 11. [CrossRef]
14. Martín-Hernández, R.; Gui, G.; Plaja, L.; Kapteyn, H.K.; Murnane, M.M.; Porras, M.A.; Liao, C.T.; Hernández-García, C. Generation of high-order harmonic spatiotemporal optical vortices. In Proceedings of the High Intensity Lasers and High Field Phenomena, Optica Publishing Group, Vienna, Austria, 12–14 March 2024; p. HW5A–6.
15. Wan, C.; Shen, Y.; Chong, A.; Zhan, Q. Scalar optical hopfions. *eLight* **2022**, *2*, 22. [CrossRef]
16. Aiello, A. Spontaneous generation of singularities in paraxial optical fields. *Opt. Lett.* **2016**, *41*, 1668–1671. [CrossRef] [PubMed]
17. Aiello, A.; Paúr, M.; Stoklasa, B.; Hradil, Z.; Řeháček, J.; Sánchez-Soto, L.L. Observation of concentrating paraxial beams. *OSA Contin.* **2020**, *3*, 2387–2394. [CrossRef]
18. Porras, M.A. Exploding paraxial beams, vortex beams, and cylindrical beams of light with finite power in linear media, and their enhanced longitudinal field. *Phys. Rev. A* **2021**, *103*, 033506. [CrossRef]
19. Mata-Cervera, N.; Sharma, D.K.; Maruthiyodan Veetil, R.; Mass, T.W.; Porras, M.A.; Paniagua-Dominguez, R. Observation of Exploding Vortex Beams Generated by Amplitude and Phase All-Dielectric Metasurfaces. *ACS Photonics* **2024**. [CrossRef]
20. Yang, Y.; Ren, Y.X.; Chen, M.; Arita, Y.; Rosales-Guzmán, C. Optical trapping with structured light: A review. *Adv. Photonics* **2021**, *3*, 034001. [CrossRef]
21. Laskin, A.; Kaiser, P.; Laskin, V.; Ostrun, A. Laser beam shaping for biomedical microscopy techniques. In Proceedings of the Biophotonics: Photonic Solutions for Better Health Care V. SPIE, Brussels, Belgium, 4–7 April 2016; Volume 9887, pp. 251–260.
22. Dunsky, C.M. Beam shaping applications in laser micromachining for the microelectronics industry. In Proceedings of the Laser Beam Shaping II. SPIE, San Diego, CA, USA, 2–3 August 2001; Volume 4443, pp. 135–149.
23. Dickey, F.M.; Lizotte, T. *Laser Beam Shaping Applications*; CRC Press: Boca Raton, FL, USA, 2017; Volume 1.
24. Wang, H.; Shi, L.; Lukyanchuk, B.; Sheppard, C.; Chong, C.T. Creation of a needle of longitudinally polarized light in vacuum using binary optics. *Nat. Photonics* **2008**, *2*, 501–505. [CrossRef]
25. Rivy, H.M.; Aljunid, S.A.; Lassalle, E.; Zheludev, N.I.; Wilkowski, D. Single atom in a superoscillatory optical trap. *Commun. Phys.* **2023**, *6*, 155. [CrossRef]
26. Strickland, D.; Mourou, G. Compression of amplified chirped optical pulses. *Opt. Commun.* **1985**, *55*, 447–449. [CrossRef]
27. Maine, P.; Strickland, D.; Bado, P.; Pessot, M.; Mourou, G. Generation of ultrahigh peak power pulses by chirped pulse amplification. *IEEE J. Quantum Electron.* **1988**, *24*, 398–403. [CrossRef]
28. Yoon, J.W.; Kim, Y.G.; Choi, I.W.; Sung, J.H.; Lee, H.W.; Lee, S.K.; Nam, C.H. Realization of laser intensity over 10^{23} W/cm^2. *Optica* **2021**, *8*, 630–635. [CrossRef]
29. Gradshteyn, I.S.; Ryzhik, I.M. *Table of Integrals, Series, and Products*; Academic Press: Cambridge, MA, USA, 1994.